Journal of Imaging Science and Technology® 57(1): 010503-1–010503-11, 2013.

Drop Speeds from Drop-on-Demand Ink-Jet Print Heads

Stephen D. Hoath▲, Wen-Kai Hsiao▲, Sungjune Jung, Graham D. Martin▲, and Ian M. Hutchings
Inkjet Research Centre, IfM, Department of Engineering, University of Cambridge, 17 Charles Babbage Road, Cambridge CB3 0FS, UK
E-mail: sdh35@cam.ac.uk

Neil F. Morrison and Oliver G. Harlen
Department of Applied Mathematics, University of Leeds, Leeds LS2 9JT, UK

Abstract. *Measured drop speeds from a range of industrial drop-on-demand (DoD) ink-jet print head designs scale with the predictions of very simple physical models and results of numerical simulations. The main drop/jet speeds at a specified stand-off depend on fluid properties, nozzle exit diameter, and print head drive amplitude for fixed waveform timescales. Drop speeds from the Xaar, Spectra Dimatix, and MicroFab DoD print heads tested with (i) Newtonian, (ii) weakly elastic, and (iii) highly shear-thinning fluids all show a characteristic linear rise with drive voltage (setting) above an apparent threshold drive voltage. Jetting, simple modeling approaches, and numerical simulations of Newtonian fluids over the typical DoD printing range of surface tensions and viscosities were studied to determine how this threshold drive value and the slope of the characteristic linear rise depend on these fluid properties and nozzle exit area. The final speed is inversely proportional to the nozzle exit area, as expected from volume conservation. These results should assist specialist users in the development and optimization of DoD applications and print head design. For a given density, the drive threshold is determined primarily by viscosity η, and the constant of proportionality k linking speed with drive above a drive threshold becomes independent of viscosity and surface tension for more viscous DoD fluid jetting:*

$$Final\_speed = k \times (Drive - Drive\_Threshold(\eta))/Nozzle\_Exit\_Area$$

[DOI: 10.2352/J.ImagingSci.Technol.2013.57.1.010503]

INTRODUCTION

Drop-on-demand (DoD) ink-jet printing successes in a widening range of industrial applications have continued to spur efforts to provide manufacturers of print heads, ink-jet fluids, and printing systems with working rules, as well as a deeper understanding of jetting processes,[1,2] that can lead to improvements. As there are many contributing, and sometimes conflicting, factors in DoD printing, one approach taken in the Cambridge, UK, Inkjet Research Centre[3] has been to use model fluids jetted from single print heads, in order to build up a better picture of key features of the problems. Most of our experimental results merely served to confirm the expectations of industrial DoD practitioners, but new insights were also gained from the high-resolution high-speed flash imaging techniques employed instead of normal strobe lighting,[4] and the development[5] of large-scale print heads to help validate DoD jetting simulations.[6] Other workers[7] beyond our UK industrial consortium have also started to exploit such results.

Our own DoD jetting simulations have been performed for the model fluids using the two-dimensional axisymmetric numerical (Leeds) code developed at the University of Leeds for viscoelastic polymers added to solvents.[8] An example of the variation in simulated jet tip speed during and after actuation by a uni-polar waveform is shown for a DoD print head nozzle of 27 μm diameter in Figure 1; the jet tip exits the nozzle at close to 10 m/s but drops down to about half of this speed. Such changes are typical for Newtonian fluids, but the details depend on actuation and geometry.

The nozzle diameter sets the timescales and break-off lengths for given drop speed and fluid properties. Figure 2 shows simulation results for a Newtonian fluid model of ultraviolet-curable ink jetting from a 50 μm diameter DoD nozzle. The target drop speed was 6 m/s and the emergent tip speed was about double this, similar to the ratio seen in Fig. 1. The simulation shows the tip/drop position with elapsed time after emergence, with the break-off time superposed. Fig. 2 demonstrates how there is a smooth transition between the tip and drop speeds at the break off for fast-moving jets. It also shows that the length of the ink-jet at break off is about 500 μm, which for this fluid and jetting speed would correspond to the lowest (minimum) stand-off distance usable in printing. Simulation results for times up to 160 μs correspond to 1 mm travel.

The great benefit of reliable jetting simulations is the ability to map a whole range of behaviors as a function of physical parameters of the fluid, e.g. density, surface tension, solvent viscosity and quality, and polymer content, as well as the geometry and size of the nozzle, and the ink-jet print head actuation drive waveform. In the present work we specifically consider fixed actuation pulse durations as typically applied for binary print heads, rather than the more complex actuation pulses for grayscale print heads, in order to produce variable volume drops. Our earlier findings,[9] based on simple observations, simulation results, and other arguments, also considered drop speed rules for more established print head technologies and applications.

▲ IS&T Members.

Received Jan. 13, 2012; accepted for publication Feb. 20, 2013; published online Apr. 23, 2013.
1062-3701/2013/57(1)/010503/11/$20.00

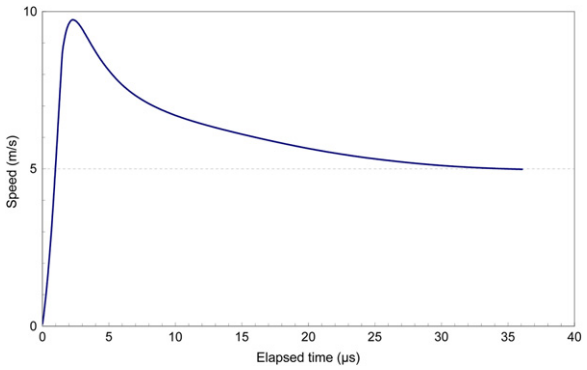

Figure 1. Simulated jet tip speed for a typical fluid jetted from a DoD print head nozzle of 27 μm diameter during and after actuation by a uni-polar waveform. The predicted ratio of peak speed to final drop speed from print heads of different nozzle sizes or manufacturers is typically ~2 for final drop speeds of ~5 m/s.

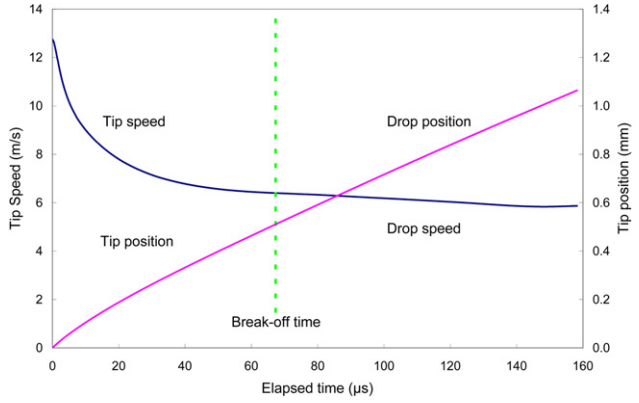

Figure 2. Simulated response for model fluid jetted from a 50 μm nozzle diameter Xaar XJ126-200 print head. The jet tip emerges initially at ~13 m/s; the ligament extends to ~0.5 mm length and breaks off ~ 67 μs later. The drop tip continues the motion, and the final speed is ~6 m/s at the ~1 mm stand-off position.

We must always consider the correspondence between results of simulation and experiments. In our simulations, the drive (boost) setting corresponds to setting up a specific velocity–time variation (waveform) behind the print head nozzle section irrespective of the fluid properties within the print head and to a certain extent the geometry of the nozzle. The fluid moves through the nozzle according to its properties and the boundary conditions within and outside the nozzle. Importantly, this means that the emergent tip speed depends on the fluid properties for a given nozzle and actuation drive. In industrial scale print heads it is not possible to determine the pressure in the print head, and therefore to establish the driving conditions in the nozzle we adjust the drive waveform to match high-resolution images of the emerging jets.

The drop speed and total jetted volume are strictly responses to the print head actuation that appear to depend linearly on the drive voltage (setting);[10] however, they are often considered as primary specifications for the DoD ink-jet printing application. Adjustments to a print head actuation waveform for a given fluid may restrict the volume printed (and hence eliminate or reduce the number of satellites produced) while achieving the required target speed. Proper fluid design may assist this process: an industrial rule of thumb regarding troubleshooting jetting issues of DoD printing is 80% fluid, 20% waveform. Most industrial printers rely on making a single adjustment, usually the amplitude of the drive voltage (setting), to achieve the drop target speed, while leaving ink specialists to provide the waveform shape. The term setting denotes any variable expected to linearly produce a corresponding drive voltage. For example, with Xaar PCI+, the software EFF value controls the drive voltage.

A Fujifilm Dimatix SX3 print head drive voltage does not directly correspond to a Xaar shared-wall drive voltage (setting) because the implementation of the piezo technology differs significantly between these manufacturers. Geometrical design differences will also influence the relationship between drive and fluid motion and hence drop speed, masking comparisons of the jetting performance. However, as the drive voltage (setting) for different print heads would most likely be linearly related between print head designs, then, despite their different scale units, relative changes in drive voltage (setting) scales can be usefully compared between print heads. We therefore attempt to generalize the findings across all DoD print heads and manufacturers.

In the present work the push, pull–push, and pull–push–pull bipolar drive waveform timescales appropriate for Dimatix, Xaar, and MicroFab print heads, respectively, were kept constant,[8] but the drive amplitude varied until achieving target drop/tip speed for all model fluids jetted. Our reported work[9] targeted ~6 m/s drop/tip speeds at ~1 mm stand-off; typical target speeds 6–8 m/s at ~0.5–2 mm stand-off distance are common in DoD applications.

Our jetting speed studies also go beyond pure Newtonian fluids, including (weakly) elastic solutions of low (<10%) concentrations of mono-disperse polystyrene in a viscous solvent. These solutions were prepared as models of high molecular weight additives to inks, and the variation of the maximum jettable concentrations was used to study the influence of polymer molecular weight across a range of different conditions, resulting[11] in the understanding of polymer regimes for high drop speed jetting and further explanations of previous results.[12,13] This work allowed us to exploit high molecular weight solutions in the same solvent which should only exhibit an enhanced Newtonian viscosity with mono-disperse polymer concentration in our jetting speed experiments, with all other properties (density and surface tension) essentially unchanged, unlike the variations occurring in conventional Newtonian water–glycerol solutions. For completeness we report drop speeds we have measured for DoD jetting of (i) pure Newtonian, (ii) weakly elastic linear polymer solutions, and (iii) shear-thinning[14] aqueous poly(3,4-ethylenedioxythiophene):(polystyrene-sulphonate) PEDOT:PSS solutions.

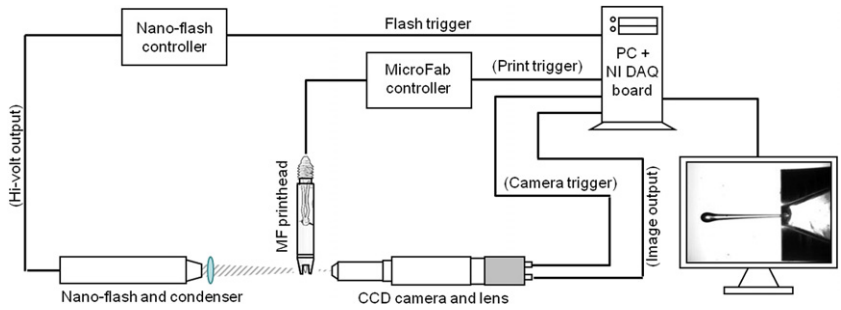

Figure 3. Example schematic for imaging of fluid jetting. (See text.) A National Instruments DAQ 6251 (i) sequences a MicroJet III controller for a MicroFab ABP print head, (ii) triggers a time-delayed ~20 ns exposure from a HSPS Nanolite spark flash, and (iii) initiates the image taking and transfer by a Prosilica CCD camera. The image on the PC screen is rotated from portrait format to allow long paths to be viewed in landscape.

EXPERIMENTS

Determinations of ink-jet drop speed, from a variety of piezo-actuated drop-on-demand (DoD) print heads, were based on image analysis of high-speed flash or high-speed video photography, as described elsewhere.[3,15] Figure 3 shows a schematic for our typical imaging apparatus comprising a High-Speed Photo-Systeme NanoLite 20 ns spark flash light source and a 10X Mitutoyo objective lens with a Navitar telescope coupled to a Prosilica CCD camera. Automated data taken from a MicroFab MJ-ABP-01 print head is depicted in Fig. 3, but other variants included jetting from Fujifilm Dimatix SX3 and Xaar XJ126-200 print heads, using Nikon D80 cameras or a Shimadzu HPV-1 ultra-high speed camera with long- duration (0.002 s) Adept Electronics flash lamp. Drop speeds were measured, by off-line image analysis, at the typical stand-off distance (between nozzle exit and substrate) of 1 mm. Calibrations of the length scales relied on optical meshes with 10 μm rulings imaged at the same magnification settings as for the jetting. Triple flash measurements (providing precisely delayed exposures of the same drop within the same image field of field) have been used to assess that the maximum image distortions were always below 2.5% and that the speed of free ~3 m/s DoD drops was almost constant (little change over a 1 mm path). Timing was measured or controlled to <0.1 μs, and the errors in timing intervals used for the drop speed determination were always <1%. Pixel resolutions used were typically ~0.5 μm, and speed measurement errors were typically <0.1 m/s.

Main drop speed determinations were made for pure Newtonian solvents, water and glycerol mixtures, shear-thinning aqueous PEDOT:PSS, and for weakly elastic linear polymer solutions of polystyrene dissolved in Newtonian solvents (diethyl or dioctyl phthalate) at various drive settings for different print heads as part of some other detailed studies[11,15–18] on these fluids.

Low-viscosity (0.002–0.0104 Pa s) water–glycerol solutions (see Table I for Newtonian fluids) and aqueous-based shear-thinning fluids[14] with surfactants were jetted to speeds >15 m/s by a 40 μm diameter MicroFab print head, for drive voltage setting steps of 5 V, as shown in Figure 4. The shear-thinning PEDOT:PSS fluids had high low shear-rate viscosity (0.012–0.060) Pa s but jet with much lower viscosity.[14]

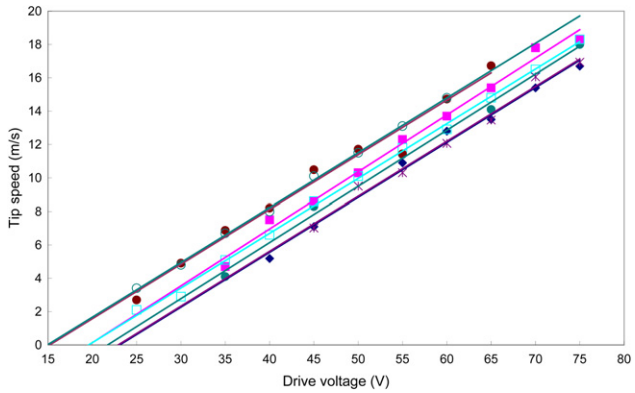

Figure 4. Measured drop speeds for low Newtonian (0.002–0.011 Pa s) viscosity water and glycerol solutions and aqueous shear-thinning PEDOT:PSS jetted from a 40 μm MicroFab nozzle.[14] The slope for each fluid appears to be reasonably linear and independent of viscosity; each fluid has a viscosity-dependent threshold voltage setting that increases with viscosity. (See the text.) Jetted Newtonian solutions with surfactants were G22W78 (○), G39W61 (●), and G60W40 (*), having the properties listed in Table I for Newtonian fluids. Aqueous PEDOT:PSS shear-thinning fluids[14] with 0.5 wt% surfactants +1 wt% (♦ and ●), 0.7 wt% (■) and 0.5 wt% (□) with effective viscosities ≤ 0.011 Pa s.

Figure 5 shows drop speeds measured from a 50 μm Xaar XJ126-200 print head with viscous fluids formed by dissolving PS (polystyrene) of specific molecular weights (e.g. PS24 is 24 kg/mol) at specific wt% (concentrations by weight) in good solvent DEP (diethyl phthalate). (See Table II of polymeric solutions for the low-shear-rate viscosities of these jetted fluids.) These polymeric fluids have been well characterized in other work[11] as producing Newtonian viscous enhancements because the relaxation times of these molecular chains are short compared with the timescales of DoD jetting, although such fluids do NOT jet in direct proportion to low-shear-rate viscosities). The drive setting shown is the (dimensionless) EFF value for the Xaar PCI+ interface, with an unspecified linear relation between EFF and the drive voltage in volts.

Figure 6 shows drop speeds for other polymeric fluids jetted[19] from a Fujifilm Dimatix SX3 27 μm diagonal square nozzle. The higher molecular weight polymeric concentrations are relatively low, and primarily contribute additional

Table I. Table for Newtonian fluids.

Designation	Name	Density (kg/m^3)	Surface tension (N/m)	Viscosity @ 25 °C (Pa s)
DEP	Diethyl phthalate	1117	0.0374	0.010
DOP	Dioctyl phthalate	980	0.0313	0.050
G22W78	Glycerol+water+surf*	1055	~0.022*	0.0019**
G39W61	Glycerol+water+surf*	1100	~0.022*	0.0036**
G60W40 @ 21 °C	Glycerol+water+surf*	1156	~0.022*	0.0104**
G60W40 @ 30 °C				0.0072
G60W40 @ 40 °C				0.0050
G60W40 @ 50 °C				0.0037
G60W40 @ 60 °C				0.0028

* 0.5% surfactants in water reduce surface tension ex ~ 0.068 N/m.
** Deduced from tables.

Table II. Table for polymeric fluids.

Designation	Concentration (wt.%)	M_w (g/mol)	PDI	Viscosity @ 25°C (Pa s)
PS24	5.0	23 800	1.02	0.0242
PS24	2.5			0.0171***
PS75	1.0	75 000	1.05	0.0147***
PS110	0.5	110 000	1.05	0.0131***
PS110	0.4			0.0125***
PS110	0.2			0.0112***
PS210	0.4	210 000	1.04	0.0127***
PS210	0.05			0.0103***
PS210	0.02			0.0101***
PS210	0.01			0.0100***
PS306	0.2	306 000	1.06	0.0122***
PS488	0.1	488 000	1.13	0.0114***

PDI is the polydispersity index, M_W/M_n, the ratio of weight-averaged molecular weight to number-averaged molecular weight for a polymer.[11]
*** Deduced from measured values of more concentrated master solutions.[11]

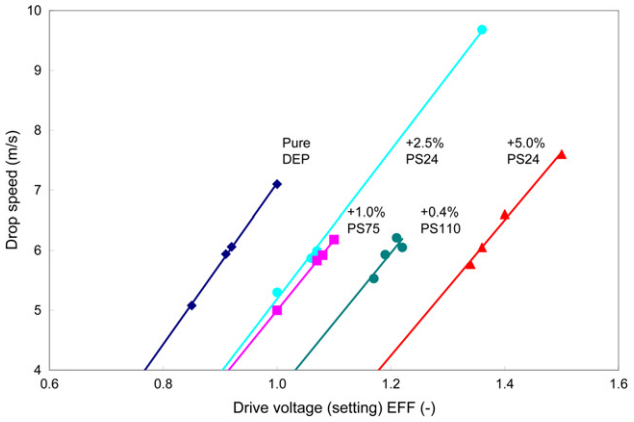

Figure 5. Drop speeds for viscous fluids jetted with the Xaar XJ126-200 print head. Jetted at ~6 m/s, these particular dilute polymer solutions are known to behave with enhanced Newtonian viscosities.[4,11] Note that the axes have offset zeros in order to better display the (sparse) data and linear fits. (See the text.)

Newtonian viscosity, although at higher concentrations in a smaller nozzle than used for this comparison they show some polymeric effects on the final jetting speed, as recently discussed elsewhere.[11] In Fig. 6, the drive voltage unit is volts.

Figure 7 shows drop speeds of relatively high concentrations of these polymeric solutions, jetted from a 30 μm MicroFab nozzle. These particular solutions had apparently well-matched linear viscoelastic properties and low-shear-rate viscosities (0.012 ± 0.01 Pa s).[20] However, while these sparse data show some semblance of a common trend, they clearly exhibit rather different speed slope and apparent threshold drive settings from the more viscous (0.016 Pa s) solvent mixture 10 wt%DOP/90wt%DEP which also jetted quite readily to far higher drop speeds. In fact the DEP + 0.1 wt% PS488 solution at 32 V reliably produced a backwards-moving main drop! The images corresponding to these jetted solutions show molecular stretching effects with increasing polymer molecular weight that are well beyond the scope of the present work.[11,21]

In most of our polymeric solution experiments, determinations of the complete range of final drop speeds were not the primary aim of the research: trial and error setting up of the print head drive gave ~6 m/s drops at the stand-off location, and henceforth the print head drive setting was held fixed. DoD practitioners will recognize that Newtonian fluids may only require 2–3 trial settings to achieve the target speed, so that not all our data were really suitable to be shown here. One reason for the (desirable) practicality of such easy setting up of a target drop speed is the very linearity in the speed versus drive voltage (setting) that we aim to explain in the present work!

As noted above, in the absence of other calibration information, any simple comparison between different print heads (for example, Figs. 5 and 6) will assume that the drive (setting) is linear in the drive voltage. We will proceed on this basis with other data throughout this article. The graphs for each print head appear to follow a similar trend, in that all drop speeds rise fairly linearly from ~1 m/s towards 10 m/s, above a threshold drive that depends strongly on the

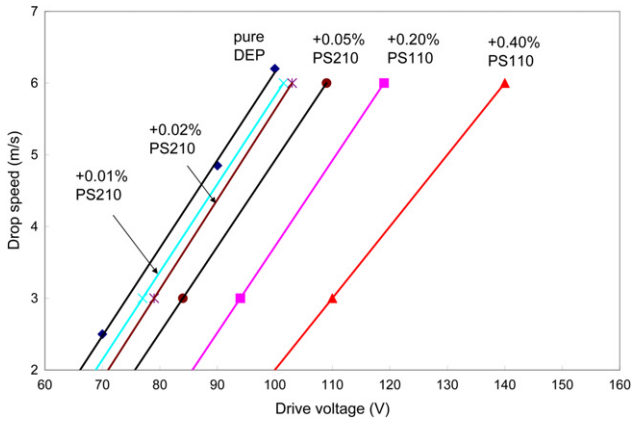

Figure 6. Drop speeds for viscous fluids jetted with the Fujifilm Dimatix SX3 print head. Low concentrations of PS110 and PS210 have slopes similar to pure DEP jetting, whereas the higher concentration of PS110 has a lower slope due to the higher elasticity of this solution, as determined previously.[11] Note that the axes have offset zeros in order to better display the (sparse) data and the linear fits. (See the text.)

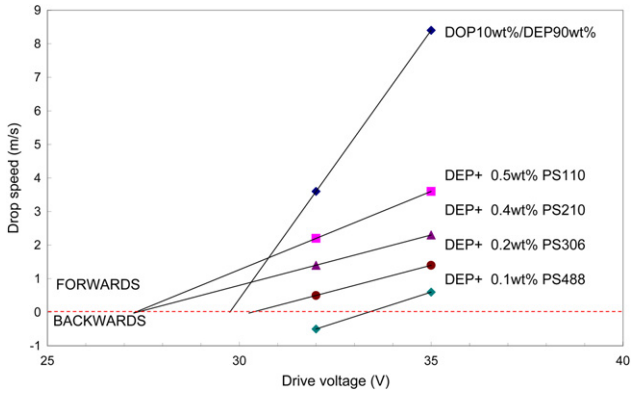

Figure 7. Drop speeds for the viscous solvent mixture 10%DOP+90%DEP and various viscoelastic fluids (matched for their low-shear-rate viscosity and linear viscoelasticity[20]) jetted using 30 μm diameter MicroFab print head nozzles. These polymeric solutions were only jetted very slowly.[21]

viscosity of the fluid with a slope that is almost independent of viscosity (at least for near-Newtonian fluids).

Anecdotal evidence from industrial ink-jet specialists and academic researchers suggests that the linear rise of speed with drive voltage (setting) is often encountered in DoD ink-jet printing with larger (>10 μm diameter) nozzles. This was also recently reported for a study of Newtonian fluid mixtures.[22] There is further information about drop speeds (e.g. measurements of air drag on droplets) available from our high- speed high-resolution imaging techniques and from other workers.[23]

This prompts consideration of the physics of DoD jetting both at slow (~0 m/s) and at faster (>2 m/s) speeds, regarding the effects of fluid properties and nozzle dimensions. Starting from empirical speed curves, through simple arguments, flow models, and simulation results, we determine whether any practical and useful scaling rules emerge for DoD ink-jet drop speeds.

Empirical modeling of jetting speed

We have reported[4] the jet tip position (s) and the speed (u) beyond the nozzle exit at time t after emergence, but before the occurrence of jet break off from the nozzle meniscus, can be well represented by simple empirical functions of the form

$$s = vt + (v_0 - v)t_0[1 - \exp(-t/t_0)] - \frac{1}{2}at^2 \quad (1)$$

$$u = v + (v_0 - v)\exp(-t/t_0) - at. \quad (2)$$

Here, v is the target tip speed ignoring the slowing-down term characterized by the constant a. Other workers[12,24] have similar formulas or data equivalent to our Eq. (1) with $a = 0$. The jet velocity at emergence from the nozzle exit is v_0, and t_0 is a characteristic timescale for the exponential decay of the tip speed towards to the target tip speed v. The emergent tip velocity v_0 is typically 2–3 times v (for an example from our DoD jetting simulations see Fig. 2 above), and t_0 for Newtonian fluids is on the same ~15 μs timescale used for the print head actuation waveform. The predicted[23] deceleration a due to air drag on a ~50 μm diameter 6 m/s drop is 110 times gravity, and opposes it for vertically oriented DoD print heads. Deceleration of the jet tip is caused by a combination of the aerodynamic drag present before and after jet break off from the meniscus, and also the surface tension, and any (non-Newtonian) elasticity present, all opposing the extending jet length before break off. Fluid viscosity also damps changes, and we have ignored the effects of external air flows, thermal changes, the presence of particulates, surfactants, shear thinning, polymer molecular chain extensibility, etc., within real ink-jet fluids.

Figure 8 shows some typical results for a Newtonian (39.5% water, 0.5% surfactants, 60% glycerol) solution jetted from a heated 40 μm diameter MicroFab nozzle. The key fluid properties depend on the temperature, and of these the viscosity is expected to most significantly influence the final drop speed. (The density changes by −2%, the viscosity by −73%, and the surface tension without surfactant changes by −7% as the fluid temperature increases from 21°C to 60°C.) The jet tip position follows Eq. (1) during the first ~100 μs of the total flight time from the nozzle exit towards the substrate, with appropriate parameters at each head temperature. The length of the image frame used in this particular study (~0.8 mm) limited the potential tracking of the higher speed leading drops (position and speed) later along the path (e.g. 1 mm stand-off).

For the rather short (~170 μs) time interval between emergence and arrival of fast ($v \sim 6$ m/s) DoD drops at the substrate ($s \sim 1$ mm), Eq. (1) shows that the slowing down term a only contributes at the <10% level (fitted $a \sim 75g$, compared with previously predicted ~110g, due to being a slightly smaller drop). For most Newtonian fluids, a has been neglected previously, whilst for some polymer solutions their larger a values are associated with elastic "bungee jumpers" that will never jet properly, i.e. never produce forward-moving drops.[10] However, it also proves possible to jet Newtonian fluids with near-zero speed, as

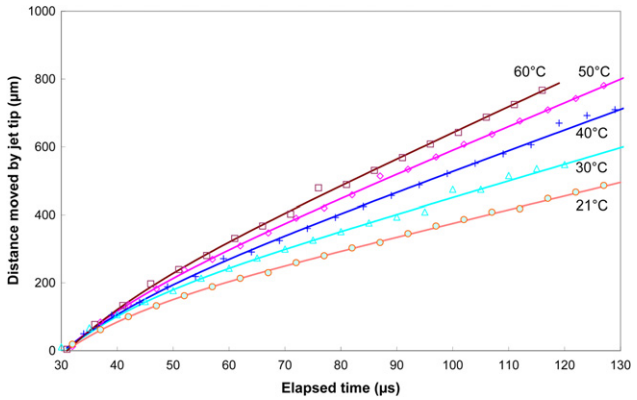

Figure 8. The distance moved by the jet tips for a Newtonian (40% water–60% glycerol) solution jetted by a heated 40 μm MicroFab print head, showing data at various head temperatures with the superposed fits to Eq. (1). All solutions were jetted with the same push–pull waveform at a fixed drive voltage (40 V). These data are shown at 5 μs steps for clarity, but the data fitted were actually measured at 1 μs steps.

we have found using high-speed cameras focused near the print head nozzle exit. Other studies[12] of polymer solutions using different DoD print head designs from those we had independently reported[4] showed that very similar empirical fitting functions to Eq. (1), but with no slowing-down term, fitted the jetting data.

All applications of DoD ink-jets involve drop formation, preferably without satellite formation, with jet break-off locations that depend on the fluid properties, nozzle diameter, jetting speed, and drive waveform used. Break-off behavior is closely related to both surface tension and viscosity, but may be inhibited by elasticity.[12] Break off is at the tail end for more viscous fluids, but immediately behind the main head for less viscous or higher surface tension fluids. Once the fluid head has broken off (some way outside the nozzle for more viscous inks[25]), any flying ligaments present will eventually retract, greatly reducing the effective length (but not the ink-jet volume) of fluid present in the jetting direction between the nozzle and the substrate.[26,27] Such behavior goes well beyond the validity of Eqs. (1) and (2)), so alternative (quantitative) approaches for understanding main DoD drop speed generation have been attempted in the present work by comparing the results of direct measurements shown in Figures 3–8 with simple physical and numerical modeling of viscous (non-elastic) fluids jetting from various DoD print heads. Jetting results for weakly elastic polymer fluids will be considered elsewhere.[21]

Simple models for flow from nozzles

Volume conservation lies at the heart of our physical models for several reasons: (1) the jetted fluids are (usually) incompressible, (2) piezo-print head actuation changes the internal volume of an ink chamber while producing ink-jets, and (3) jetting experiments with fixed (time-dependent) waveform shapes allow inter-comparisons between fluids jetted from various print head types and nozzle sizes. When comparing ink-jet drop speed with the peak drive amplitude for different nozzle exit sizes (areas), viscous DoD drop speeds ought to retain behavior arising from volume conservation suitably modified by the viscous flow constraints. This was checked by others[6] performing large-scale experiments and using numerical simulations of the print head nozzle and the fluid jets. While DoD scale experiments require accurate assessments of nozzle sizes and may suffer from differences between nozzle drive couplings, the Leeds code simulations need the nozzle shapes and sizes as inputs, a representative drive waveform, and assume that the rupture of real fluid threads must occur below a specific radial cut-off (∼1–2% nozzle width). Although an arbitrary choice of radius cut-off primarily affects the break-off times and the number of satellites formed or retained within the simulations, it does not affect the main drop speed.

For an incompressible inviscid liquid of density ρ flowing at an instantaneous volume flow rate Q through a nozzle exit of area A, the liquid slug produced in a short but finite time has an emerging tip speed which, ignoring change of shape, is linked to conservation of volume by[9]

$$Speed = Q/A. \tag{3}$$

This fluid slug will tend to change its shape from the cylindrical form into an extending jet or a drop, but we will retain the simple proportionality between speed and Q/A given in Eq. (3). For fluid flow through a DoD nozzle, the applied pressure to the fluid inside the nozzle provides the force necessary to eject the fluid out of the nozzle. This pressure is caused by piezo-actuation.[2] We now consider some details of the actuation waveform producing volume flow rate Q.

A given (time-dependent) waveform shape applied to the DoD print head produces flow rate Q at the nozzle exit. The timing (T) is kept fixed for the jetting studies, but the magnitude of the actuation can be set to different values by altering a drive voltage (setting). It can be shown by integration that the average flow rate value during a half cycle of the waveform is proportional to the peak value Q_0. For example, the average/peak is $2/\pi$ if the waveform is a half-sinusoid, 2/3 for parabolic (quadratic), and 1/2 for triangular. So, for a fixed waveform shape, the magnitude of the peak flow rate value Q_0 can represent the effects of the waveform on the fluid ejected from the nozzle. The relationship between Q_0 and the drive voltage (setting) amplitude *Drive* is usually assumed to be linear, and will be here. Although this may apply only over a restricted range of drive (setting), since power losses determined for a piezoelectric actuator were found to be quadratic in DoD drive amplitude and the efficiency of DoD print heads was estimated to be very low ∼0.07%,[2,28] others have reported that the print volume is linear in applied voltage.[10]

So, provided that the volume change Q_0T due to actuation is linear in the drive amplitude *Drive*, then Eq. (3) predicts that the jetted fluid speed is simply proportional to the amplitude of a given fixed (time-dependent) waveform shape, so a physical model prediction for DoD jetting is

$$Speed \propto Drive/A. \tag{4}$$

Eq. (4) predicts that the drop speed from all nozzles increases in proportion to the *Drive*, but the finite threshold drive (setting) values seen in Figures 3–7 are clearly inconsistent with this. Perhaps there are fluid properties that might cause this finite threshold for the given waveform. Energy has to be supplied to combat fluid inertia (density), to form new surface area (surface tension), overcome losses (viscosity), and to stretch polymeric additives (elasticity), so there are plenty of potential candidates. We consider them sequentially, starting with the surface tension, because this is the obvious choice for a stationary Newtonian fluid—no additives and low speed.

Should the flow rate Q_0 be too low or not persist long enough, then the surface tension σ acting at the ink-jet nozzle exit will tend to prevent drops from either forming or leaving the nozzle region with a usable outwards speed. This condition is reminiscent of the transition from water dripping under gravity to jetting from a faucet with increasing average flow rate Q;[29] (inviscid) jetting requires that the Weber number $We = \rho U^2 R/\sigma \geq 2$ for a nozzle radius $R = 1/2D$. This is equivalent to requiring that the fluid speed inside the nozzle is $U \geq V_T$, where $V_T = 2\sqrt{(\sigma/\rho D)}$ is the Taylor speed for retraction of a ligament of diameter D.[26] Rather similar results are found when modeling continuous ink-jet (CIJ),[30] as shown below. Therefore surface tension must provide a plausible origin for needing a finite threshold drive for jetting: surface tension considerations certainly help explain differences between Eq. (4) and jetting, but real fluids have finite viscosity and inertia, thus there are losses and fluid accelerations to consider as well: so can simple models based on Eq. (4) easily incorporate such well-known physical behavior and features?

Consider next the transient flow of a fluid having finite viscosity η within a long pipe. Flowing viscous fluids have a radially dependent velocity profile across the nozzle that alters the relationship between Q and fluid tip speed v ($\ll$ velocity of sound in fluid). Physical analysis[31] for a transient (over characteristic timescale T) viscous flow with an average speed U at Reynolds number $Re = \rho RU/\eta$ in a pipe of radius R due to pressure difference p^* across length L requires five independent dimensionless groups: geometrical (L/R); continuity (Q/UR^2) $\propto$ (Q/UA); steady flow ($p^*/\rho U^2$); transient flow (UT/L); and viscous flow (Re). The free-surface jetting analysis[29] already introduced the additional dimensionless group (We). Fluid dynamics theory suggests similar behavior whenever such groups (or finite power-law combinations of them) remain constant; here, we look at the groups for guidance with possible scaling laws for jetting. Continuity links Q/A with U and steady flow links U with $\sqrt{(p^*)}$, i.e., with $\sqrt{Drive}$.

When CIJ fluid flow is modeled[30] the formation of a liquid jet requires the creation of extra surface and hence introduces a surface energy penalty against the kinetic energy of the jet produced by the drive waveform. This energy penalty scales as surface tension σ times the surface area of the drop. For DoD, the viscosity of the fluid produces forces that depend on fluid shear rates across the size of the droplet, but are often neglected as they are expected to be smallest for the slowest drops. The extra surface energy (with $\alpha = 1$ corresponding to a new spherical surface of diameter D) for the DoD drop diameter D reduces the kinetic energy of the main drop according to

$$Final\_kinetic\_energy = Initial\_kinetic\_energy - \alpha\pi\sigma D^2. \tag{5}$$

Thus the threshold requirement for drop production ignoring viscosity is given by an exact balance of the two terms on the right-hand side of Eq. (5). The initial kinetic energy ($1/2mv_0^2$) is that corresponding to the speed in Eq. (4) and the mass contained in the diameter D of the drop. Rearranging the balance for zero final drop speed requires

$$v_0^2 = \frac{12\alpha\sigma}{\rho D} = 3\alpha v_T^2, \tag{6}$$

where the velocity v_T is the Taylor retraction speed for a fluid ligament of diameter D, which we have discussed previously:[26]

$$v_T = 2\sqrt{\frac{\sigma}{\rho D}}. \tag{7}$$

The threshold value of drop speed produced by the drive waveform needs to exceed, by a small multiple equal to $\sqrt{(3\alpha)} \sim 2$, the Taylor retraction velocity for the fluid, which depends on $1/\sqrt{D}$.

One consequence of this physical origin for the threshold for outward release of drops with a very low speed from a circular nozzle exit, to which the fluid surface is originally pinned, is that the drop diameter should be as large as the nozzle diameter, because this lowers the threshold speed v_T predicted by Eq. (7). Higher drop speed (requiring extra actuation energy and hence even higher *Drive*) is then also associated with extra volume trailing behind the drop head. Non-circular nozzles have been designed numerically to reduce the drop volume (~20%),[32] while far smaller drops can also be generated using higher radial modes across the nozzle.[2,33]

So we have established that the surface energy argument will result in DoD drops of comparable size to the nozzle diameter, as usually observed, and that there is a threshold drive value for finite main drop speed in Eq. (4), as given by Eq. (6) in terms of a known fluid parameter v_T, from Eq. (7) with D set to the size of the nozzle diameter. Rearranging our various equations to include the threshold, by modifying the linear dependence of the speed in Eq. (3) to a behavior written in terms of v_0 and the magnitude of the volume flow Q due to the waveform *Drive*, leads to Eq. (8) for given fluid properties and nozzle area A:

$$Final\_Speed = \sqrt{[Q/A]^2 - v_0^2}. \tag{8}$$

Ignoring the dependence of the drop diameter on the volume flow Q fixes v_T, and hence v_0, for given fluid

properties and nozzle area A: the curve of final speed versus the flow rate Q due to the drive waveform amplitude might be understood in terms of fluid properties and nozzle are (*Area*). Recall that the dimensionless group can link $[Q/A]^2$ with *Drive*: Eq. (8) implies that the final drop speed close to the drive threshold will not increase linearly above the drive threshold but as a square root dependence, in conflict with the observed linear increase of drop speeds. So, despite capturing a realistic DoD drop size prediction using surface tension arguments, other physical contributions to the threshold drive, arising from DoD fluid inertia, replace Eq. (8).

A more realistic assessment of DoD jetting has to consider the acceleration and maintenance of fluid speed during actuation: these speeds are driven by pressure differences across the nozzle. In particular, the dimensionless groups (UT/L) and $(p^*/\rho U^2)$ can be combined to estimate how the transient nature of DoD jetting can influence the scaling law between *Drive* and the final drop speed.

The observed experimental dependence of threshold drive setting on Newtonian fluid viscosity also requires consideration of the viscous losses in the nozzle, and we will assume both continuity and fully developed (Poiseuille) flow[31] apply for the numerical estimates provided below. The relative importance of steady and transient pressures caused by the waveform will be estimated as described by Wijshoff.[2] The usual waveforms have rise and fall times of ~2–3 μs in our work. Jetted fluid movement starts from a near-zero speed, and the fluid has typical properties of density $\rho \sim 1100$ kg/m^3, viscosity $\eta \sim 0.01$ Pa s, and surface tension $\sigma \sim 0.037$ N/m^2. So, producing drops at $U \sim 6$ m/s from a nozzle with length $L =$ nozzle and diameter $D \sim 50$ μm requires[2] a Bernoulli (kinetic energy) pressure term $1/2\rho U^2 \sim 0.2$ bar and a Newton's second law (mass × acceleration) pressure term $\rho L(dU/dt) \sim 1.9$ bar, in addition to fully developed (Poiseuille) viscous pressure term $8\pi\eta LU/A \sim 0.4$ bar and the capillary pressure term $4\sigma/D \sim 0.03$ bar. Such considerations show that surface tension only dominates for $U < 0.1$ m/s and has no effect on attainable drop speeds.

We find here that as the transient plus the viscous terms dominate, the drive pressure links linearly to the required drop speed U. In the pressure-driven regime with viscous DoD fluids, the drop speed for fixed waveform should vary linearly in drive amplitude (above threshold). This result is implicit in the extensive DoD review,[2] but we have shown here why this is important. The difference between the naïve dimensionless group expectations and the fuller treatment arise due to the inclusion of transient response in the latter: jetting always involves very rapid changes.

The origin of the experimentally observed viscosity dependence of the threshold drive setting is apparently due to the viscous losses along the finite length of the DoD nozzle. For drop speeds (typically >1 m/s) above this drive threshold setting there will be transient flow through the nozzle and associated (Poiseuille) pressure differences exceeding those due to surface tension across the nozzle exit. Extrapolating graphs of drop speed versus drive voltage setting from high speed to zero speed will reflect these viscous losses, entirely missing any surface tension effects. The actual viscous losses in jetting will differ from those calculated from fully developed flows.

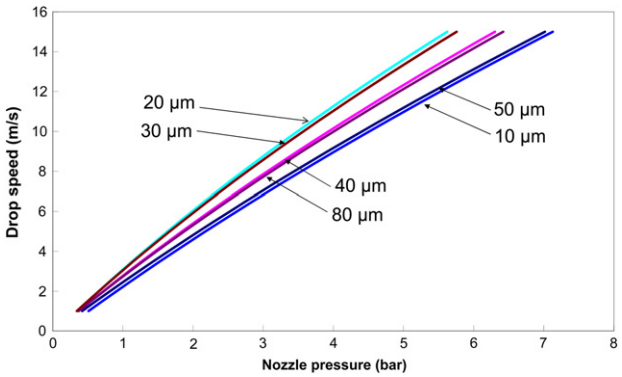

Figure 9. Curves for drop speed versus nozzle pressure for short DoD nozzle diameters as indicated. These curves were generated using the pressure terms from Wijshoff,[2] as described in the text, for a particular fluid and waveform choice. The main feature of interest here is the approximate linearity.

Figure 9 shows the predictions for DoD drop speed versus nozzle pressure, using these terms[2] for short $(L/D = 1)$ nozzles with $D = 10$, 20, 30, 40, and 50 μm and $L = 50$ μm for $D = 80$ μm. These curves suggest that a linear response may well apply for smaller sized industrial scale ink-jet drops. Although they might appear to underestimate the magnitude of the finite drive threshold for jetting seen in Figs. 3–7, these predictions are considered to be quite reasonable for push-type waveforms (as they are similar to our numerical simulation results for such waveforms).

In order to achieve 6 m/s drops, generated pressures have to reach 3 bar within the DoD nozzles; applications needing higher speed drops would require correspondingly higher internal pressures. Since pressure equals force per unit area, we can also expect, assuming that the force is linear in *Drive*, that similar drop speeds for a given actuation drive setting are reached for any nozzle size. That means that *Final_speed* should be linear in *Drive* (above threshold) divided by the nozzle area (*Area*). The constant of proportionality (k) should be similar for all fluids with the same density (ρ).

Linear extrapolation of realistic experimental drop speeds is expected to provide an apparent *Drive_Threshold* setting determined by the fluid viscosity (η) but independent of surface tension.

This implies that the final drop speed for a Newtonian fluid of given density jetted by any (fixed waveform binary) DoD print head could be expected to follow the empirical equation (9):

$$Final\_speed = k(Drive - Drive\_Threshold(\eta))/Area. \quad (9)$$

The empirical equation (9) ignores the effects of surface tension for drop speeds >1 m/s; the 'slope' coefficient k is independent of viscosity, while the drive threshold depends

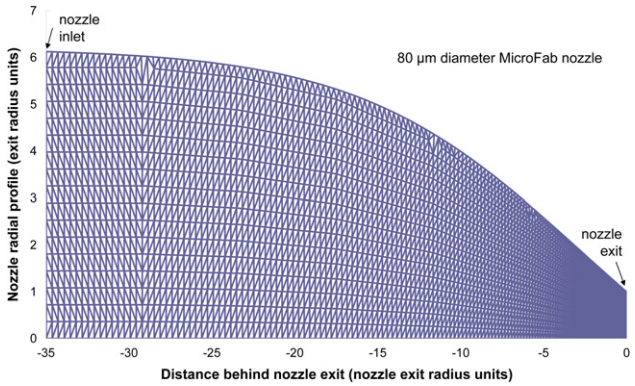

Figure 10. Two-dimensional axisymmetric mesh generated for the Leeds numerical simulations of an 80 μm diameter DoD MicroFab nozzle, based on our measurements of the nozzle profile,[16] in dimensionless units.

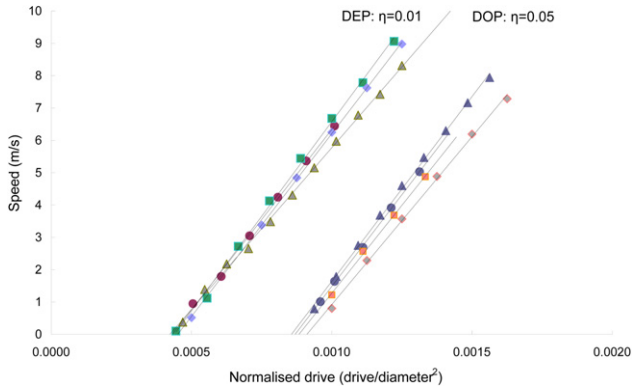

Figure 11. Showing the results of simulations of viscous fluid jetting for the MicroFab (MF) nozzle with various nozzle exit diameters. DEP has a viscosity of 0.01 Pa s and DOP has a viscosity of 0.05 Pa s. The simulations are for MicroFab nozzles with (▲) 80, (●) 50, (■ 30, and (♦) 20 μm exit diameters, using the measured radial profile for each nozzle to form the appropriate mesh for the jetting simulations. The normalized drive setting equals the mesh inlet velocity wave amplitude divided by (nozzle diameter D)^2.

on viscosity. This useful rule for DoD drop speed predictions was first proposed at NIP27 (in 2011).[9] In addition, the slope coefficient k may linearly depend on density (from dimensionless group ideas) and the drive threshold also depends on the waveform type (greater for pull–push than for push).

Numerical simulations of Newtonian fluid jetting

A common waveform used here for a particular set of simulations was deduced from our particle image velocimetry (PIV) measurements on an 80 μm diameter MicroFab nozzle.[16] Other waveform profiles produced a similar pattern of drop speeds versus drive voltage (setting). Newtonian fluids with similar Weber number but different viscosities typical of the range encountered in DoD printing were chosen for simulation: DEP (diethyl phthalate $\eta = 0.010$ Pas) and DOP (dioctyl phthalate $\eta = 0.050$ Pas). We simulated the MicroFab drop speed variation with nozzle exit diameter because this can help check the flow model predictions of Eq. (9).

Each MicroFab nozzle shape (an example for an 80 μm diameter exit is shown in Figure 10) was pre-measured[25] in order to generate realistic axisymmetric mesh geometry within the nozzles for the numerical simulations. The radial profile $R(z)$ at distance z (for $z \leq 0$ in units of the nozzle exit radius) was fitted to the smooth expression

$$R(z) = \frac{1}{2}\left\{R_1 + R_2 + (R_1 - R_2)\tanh\left(\frac{z - z_1}{z_0}\right)\right\}. \quad (10)$$

The central location of the profile shape is at $z = z_1$, and the width of the transition is z_0, while $R_2 = R(-\infty) \approx$ nozzle inlet radius, and $R_1 = R(+\infty)$ is a (negative) empirical fit parameter to reproduce the nozzle exit radius $R(0)$.

Figure 11 shows results from the numerical simulations of various sizes of MicroFab nozzle. The final drop speed is shown (up to at least 6 m/s) to rise roughly linearly above a threshold value for the normalized drive, which is the simulation drive voltage setting (amplitude applied to a common waveform) divided by the square of the nozzle exit diameter. Recall that this normalization is equivalent to the pressure produced by the actuation, independent of exit radius, and therefore is proportional to the x-axis in Fig. 9. The results cluster around normalized drive thresholds which depend significantly on viscosity and also respect the conservation of fluid volume while approximating to the empirical equation (9) for the fluid viscosities and DoD nozzles considered.

Figure 12 shows the predicted DoD drive threshold settings obtained by numerical simulations for 80 μm diameter MicroFab nozzles jetting a range of Newtonian fluids with the key properties in the normal range (surface tension 0.012–0.074 N/m and viscosity 0.003–0.050 Pa s). The predicted drive threshold settings are almost linear in, and rather weakly dependent on, surface tension, compared with the influence of the fluid viscosity, as suggested by Eq. (9). While the quality of the fits does not discriminate between linear or power law in surface tension, we anticipate that a linear law will be more realistic due to finite density for all these simulations.

Figure 13 shows the predicted slope $\Delta U/\Delta V$, for the change of drop speed with DoD drive (voltage) setting above the threshold drive setting obtained from the simulations in Fig. 12. The slope for the most viscous (0.05 Pa s) fluid simulated is practically independent of surface tension, and may provide an operating point for applications where dynamic surface tension is deleterious. However, the majority of DoD systems are operated at far lower viscosities (typically around 0.01 Pa s, achieved by heating the fluid in the print head) to avoid the extra drive required to beat the jetting threshold, and as a result they become sensitive to lower values of surface tension (typically 0.012–0.025 N/m), which are commonly preferred in applications.

Other simulations have been run with push rather than pull–push waveforms to show that the drive threshold required to jet fluid is reduced in the former case. Simulations also revealed a push slope coefficient with negligible

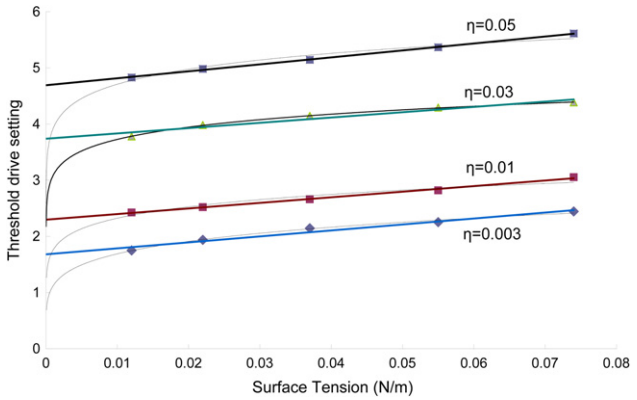

Figure 12. Drive threshold setting (arbitrary units) for 80 μm MicroFab nozzles, simulated for fluids of various surface tensions and at four stated viscosities (Pa s) fitted by straight lines or by simple power laws. Threshold drive settings for these four are almost linear in surface tension between 0.012 and 0.074 N/m.

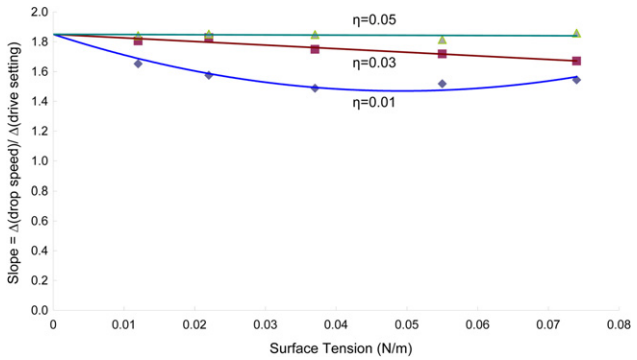

Figure 13. Slope of drop speed with drive voltage setting above threshold versus surface tension generated by simulation for various fluid viscosities (0.01, 0.03, and 0.05 Pa s), with solid curves shown to guide the eye. These results are for the 80 μm MicroFab print head simulation using the measured DoD waveform.[16]

dependence on density, viscosity, or surface tension, but with a slight dependence on the exit diameter size for the tapering MicroFab nozzle geometry. The area-normalized threshold drives required for each of these simulation cases were similar but also increased as low power-law functions of surface tension (about 0.2) and viscosity (0.4–0.45). Such power-law dependences would not readily emerge from the simple modeling, but such trends might be anticipated from the discussion we have provided, short of direct measurements.

Our empirical equation (9), in combination with detailed numerical simulations, may suggest alternative solutions in applications which could benefit from less sensitivity to surface tension while accommodating a more viscous jetting fluid, e.g. by choosing a lower jetting temperature, and doubtless other opportunities for exploiting the empirical equation will occur to practitioners.

DISCUSSION

When the drop speed data for jetting pure DEP are compared between different print head manufacturers and nozzle diameters, in units of the apparent threshold drive the drop speed increases by 5–6 m/s per unit of drive above the threshold drive. This result arises from the common fluid and piezoelectric actuation used, while the speeds are measured to far better than ±1 m/s. The simulations presented in the present work were not intended to be directly compared with experiments but to provide guides to the speed trends with fluid properties and nozzle diameters. We subsequently found by varying the waveform from pull–push to push type that the threshold drive could be lowered significantly without changing the slope of the speed versus drive curve. Our simulation results for DEP jetted by the MicroFab print head predict that speeds would increase by 15 m/s per unit of drive above the threshold drive. This discrepancy with the observed data suggests that our threshold drive predictions for the MicroFab using a pull–push waveform are too high. No such problems have been encountered for short DoD nozzles.[6–8] One possible explanation is that bidirectional waves produced within the MicroFab print head[10] reinforce to provide fluid motions not properly accounted for in our numerical simulations, since this might suggest (by halving the threshold) an increase by 7.5 m/s per unit of threshold drive, which would be far closer to the experimental speeds and perhaps within experimental errors.

CONCLUSIONS

The experimental results for different fluid types, DoD nozzles, and manufacturing technologies, together with flow modeling and numerical simulations of fluid jetting, show that jet speed trends with nozzle diameters, fluid viscosities, and drive amplitudes are predictable. This knowledge should be helpful for applications. The Newtonian simulation results are also reasonably consistent with measurements of drop speed measured with PS+DEP fluids that are weakly viscoelastic. Very simple guidelines suggested by the fundamental fluid dynamics behavior of inviscid CIJ jets from nozzles do not explain DoD jetting of fluid with higher viscosity. The general results for DoD jetting with a given waveform timing is that the Newtonian fluid drop speed is linear in the drive setting above a threshold that is independent of the nozzle exit diameter but which does depend significantly on the viscosity of the fluid. The final speed variation with drive is generally inversely proportional to the square of the nozzle exit diameter (due to volume conservation, and as it should if actuation drive setting linearly produces a nozzle pressure within the print head). At higher DoD viscosities the slope of this variation is a constant independent of surface tension. At lower DoD fluid viscosities, the slope depends on surface tension: this altered sensitivity is significant for implementation of practical DoD jetting. We have demonstrated the utility of a combination of jetting measurements, modeling, and numerical simulation in providing technical guidance for DoD applications and print head developments, encapsulated by our equation (9).

ACKNOWLEDGMENTS

This work was supported by our industrial partners and the UK EPSRC through grant number GR/T11920/01

(Next Generation Ink-jet Printing) and grant number EP/H018913/1 (Innovation in Industrial Ink-jet Technology). Tri Tuladhar is thanked for his comments, and we acknowledge our academic partners at the Universities of Cambridge, Durham, Leeds, and Manchester, and our industrial partners for helpful discussions and permission to publish these research findings. The EPSRC Engineering Instrument loan pool provided access to ultra high speed cameras used for some of this work.

REFERENCES

[1] J. F. Dijksman, "Hydrodynamics of small tubular pumps," J. Fluid Mech. **139**, 173 (1984).
[2] H. Wijshoff, "The dynamics of the piezo inkjet print head operation," Phys. Rep. **491**, 77–177 (2010).
[3] I. M. Hutchings, G. D. Martin, and S. D. Hoath, "High speed imaging and analysis of jet and drop formation," J. Imaging Sci. Technol. **51**, 438–444 (2007).
[4] S. D. Hoath, I. M. Hutchings, G. D. Martin, T. R. Tuladhar, M. R. Mackley, and D. C. Vadillo, "Links between fluid rheology and drop-on-demand jetting and printability," J. Imaging Sci. Technol. **53**, 041208 (2009) 8pp.
[5] J. R. Castrejón-Pita, G. D. Martin, S. D. Hoath, and I. M. Hutchings, "A simple large-scale droplet generator for studies of inkjet printing," Rev. Sci. Instrum. **79**, 075108 (2008).
[6] J. R. Castrejón-Pita, N. F. Morrison, O. G. Harlen, G. D. Martin, and I. M. Hutchings, "Experiments and Lagrangian simulations on the formation of droplets in drop-on-demand mode," Phys. Rev. E **83**, 036306 (2011).
[7] E. Kim and J. Baek, "Numerical study on the effects of non-dimensional parameters on drop-on-demand droplet formation dynamics and printability range," Phys. Fluids **24**, 082103 (2012).
[8] N. F. Morrison and O. G. Harlen, "Viscoelasticity in inkjet printing," Rheologica Acta **49**, 619 (2009).
[9] S. D. Hoath, W.-K. Hsiao, S. Jung, G. D. Martin, and I. M. Hutchings, "Dependence of drop speed on nozzle diameter, viscosity and drive amplitude in drop-on-demand ink-jet printing," *Proc. IS&T's NIP27: Int'l. Conf. on Digital Printing Technol. and Digital Fabrication 2011* (IS&T, Springfield, VA, 2011) pp. 62–65.
[10] N. Reis, C. Ainsley, and B. Derby, "Ink-jet delivery of particle suspensions by piezoelectric droplet ejectors," J. Appl. Phys. **97**, 094903 (2005).
[11] S. D. Hoath, O. G. Harlen, and I. M. Hutchings, "Jetting behavior of polymer solutions in drop-on-demand inkjet printing," J. Rheology **56**, 1109–1127 (2012); S. D. Hoath, I. M. Hutchings, O.G. Harlen, C. McIlroy and N. F. Morrison, "Regimes of polymer behaviour in drop-on-demand ink-jetting," *Proc. IS&T's NIP28: Int'l. Conf. on Digital Printing Technol. and Digital Fabrication 2012* (IS&T, Springfield, VA, 2012) pp. 408–411; C. McIlroy, O.G. Harlen, and N.F. Morrison, "Modelling the jetting of dilute polymer solutions in drop-on-demand inkjet printing", submitted to J. Non-Newt. Fluid Mech. (2012).
[12] B. J. de Gans, E. Kazancioglu, W. Meyer, and U. S. Schubert, "Inkjet printing polymers and polymer libraries using micropipettes," Macromol. Rapid Commun. **25**, 292–296 (2004); B. J. de Gans, L. J. Xue, U. S. Agarwal and U. S. Schubert, "Ink-jet printing of linear and star polymers," Macromol. Rapid Commun. **26**, 310–314 (2005).
[13] K. A-Alamry, K. Nixon, R. Hindley, J. A. Odell, and S. G. Yeates, "Flow-induced polymer degradation during ink-jet printing," Macromol. Rapid Commun. **32**, 316–320 (2011).
[14] S. D. Hoath, S. Jung, W.-K. Hsiao, and I. M. Hutchings, "How PEDOT:PSS solutions produce satellite-free inkjets," Organic Electron. **13**, 3259–3262 (2012).
[15] S. Jung and I. M. Hutchings, "The impact and spreading of a small liquid drop on a non-porous substrate over an extended timescale," Soft. Matter **8**, 2686–2696 (2012).
[16] J. R. Castrejón-Pita, S. D. Hoath, A. A. Castrejón-Pita, N. F. Morrison, W.-K. Hsiao, and I. M. Hutchings, "Time-resolved particle image velocimetry within the nozzle of a drop-on-demand print-head," J. Imaging Sci. Technol. **56**, 050401 (2012); J. R. Castrejón-Pita, S. D. Hoath, A. A. Castrejón-Pita, N. F. Morrison, W.-K. Hsiao and I. M. Hutchings, "Ultra-high speed particle image velocimetry on drop-on-demand jetting," *Proc. IS&T's NIP27: Int'l. Conf. on Digital Printing Technol. and Digital Fabrication 2011* (IS&T, Springfield, VA, 2011) pp. 93–96.
[17] D. C. Vadillo, T. R. Tuladhar, A. C. Mulji, S. Jung, S. D. Hoath, and M. R. Mackley, "Evaluation of ink jet fluids performance using the Cambridge Trimaster filament stretch and break-up device," J. Rheology **54**, 261 (2010).
[18] D. C. Vadillo, S. D. Hoath, W.-K. Hsiao, and M. R. Mackley, "The effect of inkjet ink composition on rheology and jetting behavior," *Proc. IS&T's NIP27: Int'l. Conf. on Digital Printing Technol. and Digital Fabrication 2011* (IS&T, Springfield, VA, 2011) pp. 568–572.
[19] S. Jung, S. D. Hoath, and I. M. Hutchings, "The role of viscoelasticity in drop impact and spreading for inkjet printing of polymer solution on a wettable surface," Microfluid. Nanofluid. **14**, 163–169 (2013).
[20] D. C. Vadillo, W. Mathues, and C. Clasen, "Microsecond relaxation processes in shear and extensional flows of weakly elastic polymer solutions," Rheologica Acta **51**, 755–769 (2012).
[21] S. D. Hoath, D. C. Vadillo, T. R. Tuladhar, S. Jung, W.-K. Hsiao, G. D. Martin, and I. M. Hutchings, Ink-jet printing of weakly elastic polymer solutions, in submission to Journal of Non-Newtonian Fluid Mechanics (2013).
[22] L. Y. Wong, G. H. Lim, T. Ye, F. B. S. Silva, J. M. Zhuo, R. Q. Png, S. J. Chua, and P. K. H. Ho, "Jettable fluid space and jetting characteristics of a microprint head," J. Fluid Mech. **713**, 109–122 (2012).
[23] M. M. Mohebi and J. R. G. Evans, "The trajectory of ink-jet droplets: modeling and experiment," Chem. Engng Sci. **60**, 3469–3476 (2005).
[24] A.-S. Yang, C. H. Cheng, and C.-T. Lin, "Investigation of droplet-ejection characteristics for a piezoelectric inkjet printhead," Proc. IMechE Part C: J. Mech. Engng Sci. **220**, 435–445 (2005).
[25] S. D. Hoath, G. D. Martin, and I. M. Hutchings, "Effects of fluid viscosity on DoD ink-jet break-off," *Proc. IS&T's NIP26: Int'l. Conf. on Digital Printing Technol. and Digital Fabrication 2010* (IS&T, Springfield, VA, 2010) pp. 10–13.
[26] S. D. Hoath, G. D. Martin, and I. M. Hutchings, "A model for jet shortening in drop-on-demand ink jet printing," *Proc. IS&T's NIP25: Int'l. Conf. on Digital Printing Technol. and Digital Fabrication 2009* (IS&T, Springfield, VA, 2009) pp. 75–78; S. D. Hoath, G. D. Martin and I. M. Hutchings, "Improved models for DoD ink-jet shortening," *Proc. IS&T's NIP26: Int'l. Conf. on Digital Printing Technol. and Digital Fabrication 2010* (IS&T, Springfield, VA, 2010) pp. 353–355.
[27] S. D. Hoath, S. Jung, and I. M. Hutchings, "Simple criterion for jet break up in drop-on-demand inkjet printing," Phys. Fluids **25**, 021701 (2013).
[28] D. Cibis and K. Kruger, "System analysis of a DoD print head for direct writing of conductive circuits," Int'l. J. Appl. Ceramic Technol. **4**, 428 (2007).
[29] C. Clanet and J. C. Lasheras, "Transition from dripping to jetting," J. Fluid Mech. **383**, 307–326 (1999).
[30] W. van Hoeve, S. Gekle, J. H. Snoeijer, M. Versluis, M. P. Brenner, and D. Lohse, "Breakup of diminutive Rayleigh jets," Phys. Fluids **22**, 122003 (2010) equation (1) therein.
[31] T. E. Faber, *Fluid Dynamics for Physicists* (Faber, Cambridge UK, 1995). Chapter 1, equations (1.10) and (1.36) therein.
[32] H. H. Chen and M. P. Brenner, "The optimal faucet," Phys. Rev. Lett. **92**, 166106 (2004).
[33] A. U. Chen and O. A. Basaran, "A new method for significantly reducing drop radius without reducing nozzle radius in drop-on-demand drop production," Phys. Fluids **14**, L1 (2002).